PROCEEDINGS OF SPIE

Fine-pitch and thick-foil gas electron multipliers for cosmic x-ray polarimeters

Toru Tamagawa, Asami Hayato, Yorito Yamaguchi, Hideki Hamagaki, Shigehira Hashimoto, et al.

SPIE.

Fine-pitch and thick-foil gas electron multipliers for cosmic x-ray polarimeters

Toru Tamagawa[a,b], Asami Hayato[b,a], Yorito Yamaguchi[c], Hideki Hamagaki[c],
Shigehira Hashimoto[b,a], Masahide Inuzuka[d], Hiromasa Miyasaka[e], Ikuya Sakurai[f],
Fuyuki Tokanai[g], Kazuo Makishima[h,a]

[a]RIKEN, The Institute of Physical and Chemical Research, 2-1 Hirosawa, Wako,
Saitama 351-0198, Japan;
[b]Department of Physics, Tokyo University of Science, 1-3 Kagurazaka,
Shinjyuku-ku, Tokyo 162-8601, Japan;
[c]Center for Nuclear Study (CNS), University of Tokyo, 2-1 Hirosawa, Wako,
Saitama 351-0198, Japan;
[d]National Research Institute for Cultural Properties, Tokyo, 13-43 Ueno Park,
Taito-ku, Tokyo 110-8713, Japan;
[e]Caltech, MC 220-47, Pasadena, CA 91125, USA;
[f]EcoTopia Science Institute, Nagoya University, Furo-cho, Chikusa, Nagoya,
Aiti 464-8603, Japan;
[g]Department of Physics, Yamagata University, 1-4-12 Kojirakawa,
Yamagata 990-8560, Japan;
[h]Department of Physics, University of Tokyo, 7-3-1 Hongo, Bunkyo-ku,
Tokyo 113-0033, Japan

ABSTRACT

We have produced various gas electron multiplier foils (GEMs) by using laser etching technique for cosmic X-ray polarimeters. The finest structure GEM we have fabricated has 30 μm-diameter holes on a 50 μm-pitch. The effective gain of the GEM reaches around 5000 at the voltage of 570 V between electrodes. The gain is slightly higher than that of the CERN standard GEM with 70 μm-diameter holes on a 140 μm-pitch. We have fabricated GEMs with thickness of 100 μm which has two times thicker than the standard GEM. The effective gain of the thick-foil GEM is 10^4 at the applied voltage of 350 V per 50 μm of thickness. The gain is about two orders higher than that of the standard GEM. The remarkable characteristic of the thick-foil GEM is that the effective gain at the beginning of micro-discharge is quite improved. For fabricating the thick-foil GEMs, we have employed new material, liquid crystal polymer (LCP) which has little moisture absorption rate, as an insulator layer instead of polyimide. One of the thick-foil GEM we have fabricated has 8 μm copper layer in the middle of the 100 μm-thick insulator layer. The metal layer in the middle of the foil works as a field-shaper in the multiplication channels, though it slightly decreases the effective gain.

Keywords: Cosmic X-ray Polarimeter, gas electron multiplier, GEM, proportional counter

1. INTRODUCTION

The gas electron multiplier (GEM) foil has been developed at CERN since the pioneering work by Sauli in 1996.[1] The basic structure of the GEM is that small, densely packed holes are drilled through copper-plated polyimide. When a potential difference is applied between the two copper electrodes in a suitable gas, the foil works as an electron multiplier of a proportional counter. Recently, GEM foils have been used in many applications, such as particle tracking,[2] photon detectors,[3–5] X-ray imagers.[6]
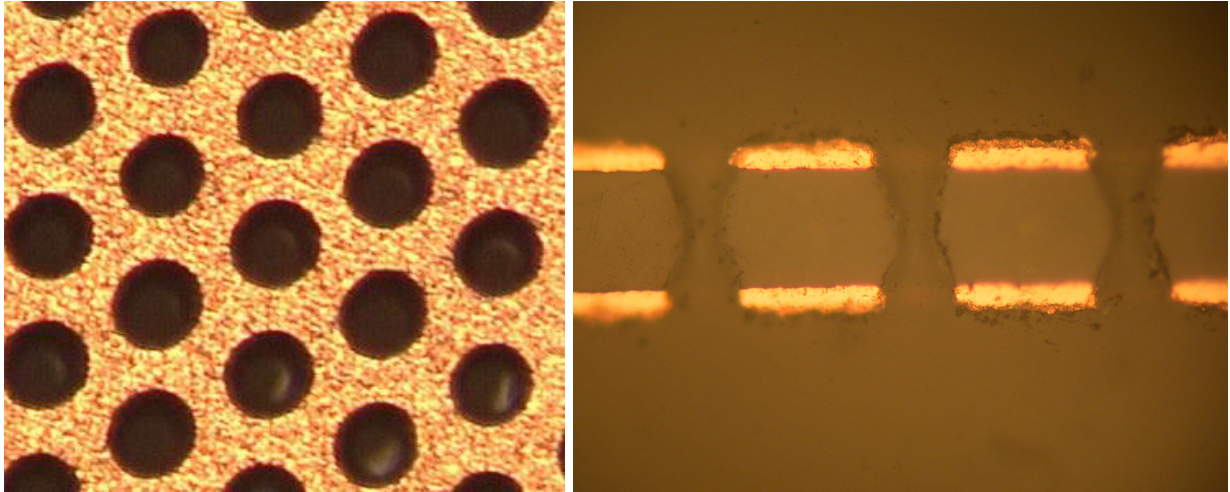

Figure 1. (Left) Magnified surface image of the laser etched GEM with pitch of 50 μm and hole diameter of 30 μm. (Right) Cross section of the GEM with thickness of 50 μm.

We are interested in applying the GEMs to cosmic X-ray polarimeters in which GEMs are combined with fine pixel array detectors.[7–10] Based on the photoelectric effect, polarization of the incident X-ray is obtained by determining the emission angle of the photoelectron, which is correlated with the electric field vector of the X-ray. The key to increasing analyzing power is to accurately trace the photoelectron path, which is only about 1 mm even in neon at atmospheric pressure for 5 keV X-ray,[11] though there is no sense in making pixels smaller than the lateral diffusion of drift electrons. If we carefully chose a gas and a depth of the drift region in order to extract the highest possible modulation, the pixel size is found to be 50-100 μm.[12]

It is, however, difficult to produce a stable, high-gain GEM with a pitch less than 100 μm for 50 μm-thick foil using the standard chemical etching technique. Therefore, we have pursued another technique for drilling the polyimide.[13] The laser etching technique is the most promising method to produce fine pitch GEMs. Recently, we have produced the GEMs by using CO_2 laser etching.[14] The laser etching was originally employed by J. Benlloch et al.[15] and some other efforts were reported.[9, 16, 17]

When we fabricate the fine-pitch GEMs, thinner foil is better for drilling polyimide properly. However, thicker foil is better for high-gain GEMs. Our goal is, therefore, to produce fine-pitch GEMs with thick-foil stably. In this paper, we present current status of our GEM productions and properties of the GEMs.

2. PRODUCTION OF FINE-PITCH AND THICK-FOIL GEMS

2.1. Fine-pitch GEMs

So far, the finest structure GEM we have fabricated has 30 μm-diameter holes on a 50 μm-pitch. The base plate is 50 μm-thick polyimide sandwiched by two 5 μm-thick copper layers. Fig. 1 shows the surface and cross section image of the 50 μm-pitch GEM drilled by the CO_2 laser. The hole is slightly double conical shape with small taper angle of less than 10 degrees. The taper is slightly shallower than that of CERN standard GEMs.

We used six different types of GEMs in this work, listed in Table 1. The so-called "standard GEM" fabricated by the CERN-GDD group[18] using chemical etching with a pitch of 140 μm and a hole diameter of 70 μm, is called CERN-140. The same geometry as CERN-140 made with CO_2 laser etching is designated as RIKEN-140. The CO_2 laser-etched GEM fabricated by us with a pitch of 50 μm and a hole diameter of 30 μm is called RIKEN-50. All of the above GEMs have 5 μm-thick copper electrodes and a 50 μm-thick polyimide layer. Each GEM has 30×30 mm^2 active area. The other three types of GEMs are mentioned in the next subsection.

2.2. Thick-foil GEMs

We have produced the GEMs with liquid crystal polymer (LCP) as an insulator instead of polyimide. One of the shortcomings of the polyimide is its moisture absorption. The absorption of moisture during the GEM production process causes transformation of polyimide layer into wavy shape. To avoid the transformation, we have employed LCP. While typical moisture absorption is 1.5% for polyimide in the atmosphere at 25 °C with 50% humidity, the moisture absorption is less than 0.04% for LCP.[19] In addition, contamination of water vapor from the detector materials causes serious problem, which lowers the gas gain, for gas counters. We can reduce the contamination if we use LCP.

In this work we used three different types of GEMs produced with LCP. One of them has 50 μm-thick foil with hole diameter of 70 μm and pitch of 140 μm, called RIKEN-140LCP. Second has the same hole diameter and pitch, but the thickness is 100 μm, called RIKEN-140LCP-100T. The last one has also the same hole diameter and pitch, but an 8 μm-thick copper layer is sandwiched by two 50 μm-thick LCP layers and two 8 μm-thick copper layers are plated on both side of the LCP-Cu-LCP layer. The last one called RIKEN-140LCP-2L. The cross sections of RIKEN-140LCP, RIKEN-140LCP-100T, and RIKEN-140LCP-2L are shown in Fig. 2. Each GEM has also 30×30 mm^2 active area. All of the RIKEN GEMs listed in the Table 1 were designed at RIKEN and fabricated by Scienergy Co. Ltd. *

Table 1. List of GEM foils examined in this study. All dimensions are given in μm. The fourth column shows the thickness of only the insulator layers. The copper electrodes have 5 μm in thickness for copper plated polyimide and 8 μm for the copper plated liquid crystal polymer.

name	pitch	hole dia.	thickness	insulator	etching method
CERN-140	140	70	50	polyimide	chemical
RIKEN-140	140	70	50	polyimide	CO_2 laser
RIKEN-50	50	30	50	polyimide	CO_2 laser
RIKEN-140LCP	140	70	50	liquid crystal polymer	CO_2 laser
RIKEN-140LCP-100T	140	70	100	liquid crystal polymer	CO_2 laser
RIKEN-140LCP-2L	140	70	50×2layer	liquid crystal polymer	CO_2 laser

3. PROPERTY OF THE GEMS

3.1. Experimental Setup

Fig. 3 shows a schematic view of the GEM test setup. It consists of a drift plane, GEM foils, and 3×3 readout pads with each area of 10×10 mm^2. Only the central readout pad was read out in the study and the other pads were connected to ground. The drift plane is 15 μm-thick aluminum foil with active area of 30×30 mm^2. The drift plane, GEMs, and readout pads are placed in a gas filled chamber. The spacing between the drift plane and the upper GEM (i.e. the spacing of target region) is 5.5 mm, and that between the lower GEM and readout pad is 1.0 mm. The electric field in the drift region is E$_d$=2.5 kV/cm, and E$_i$=4∼5 kV/cm for the induction region. A GEM is often used as a preamplifier to the other GEM to reduce discharge probability and ion feedback.[20] When we studied the GEMs in the multi layer configuration, the spacing among GEMs was 2.0 mm with electric field of E$_t$ ∼2 kV/cm. We did not take care to align GEMs in this study because transverse diffusion in the gap exceeds the pitch of the GEM holes. The high voltage is supplied via a chain of 10 MΩ resistors, and a 2 MΩ protection resistor is added in series with each GEM electrode.

Charge signals from the readout pads are fed into a charge sensitive preamplifier and shaper module (AmpTek A225). The amplified and shaped voltage signals are fed into the custom-made main amplifier. This module has a discriminator and gate generator for data acquisition system control. The amplified signals are fed into

---

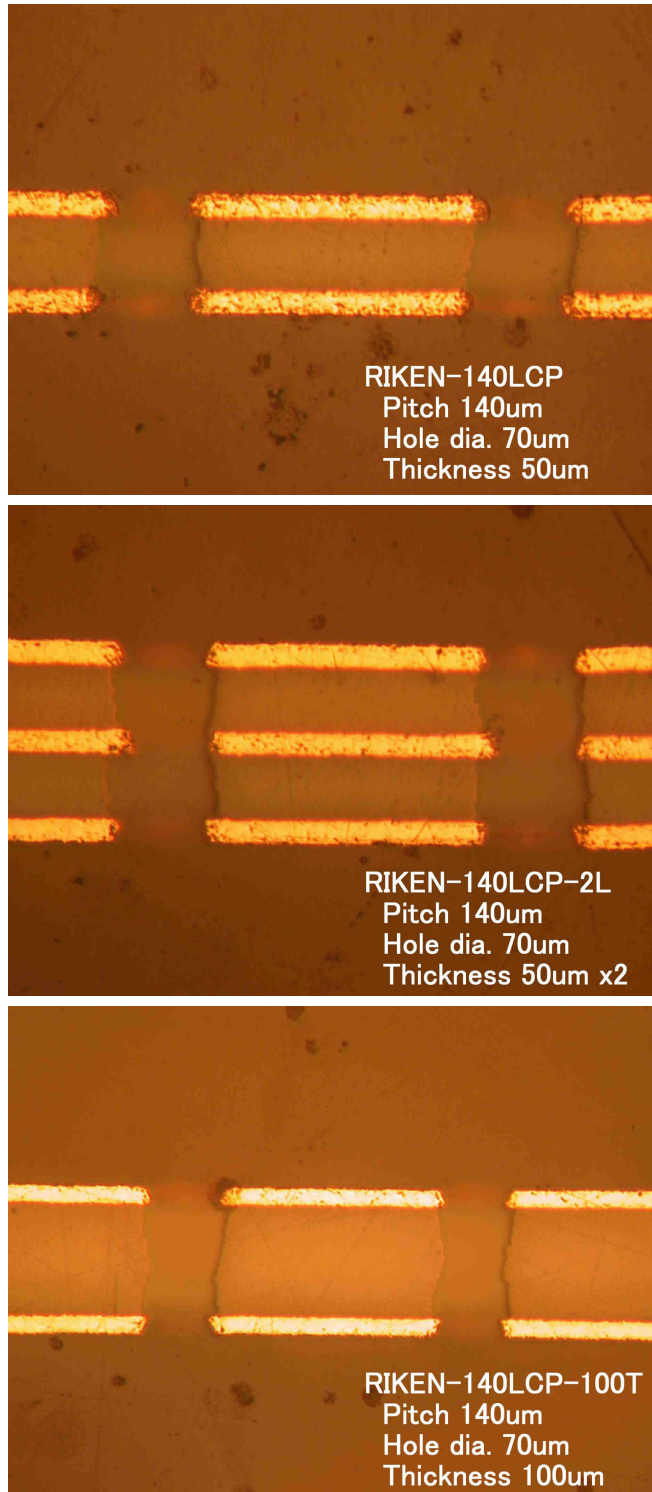*Contact address of Scienergy Co. Ltd. is info@scienergy.jp.

Figure 2. (Upper) The cross section of the RIKEN-140LCP GEM with pitch of 140 μm and hole diameter of 70 μm. The insulator between the copper layers is LCP with thickness of 50 μm. (Middle) The cross section of RIKEN-140LCP-2L. There is the 8 μm-thick copper layer in the middle of the insulator layer. (Lower) The cross section of the RIKEN-140LCP-100T GEM with 100 μm-thick LCP laser.
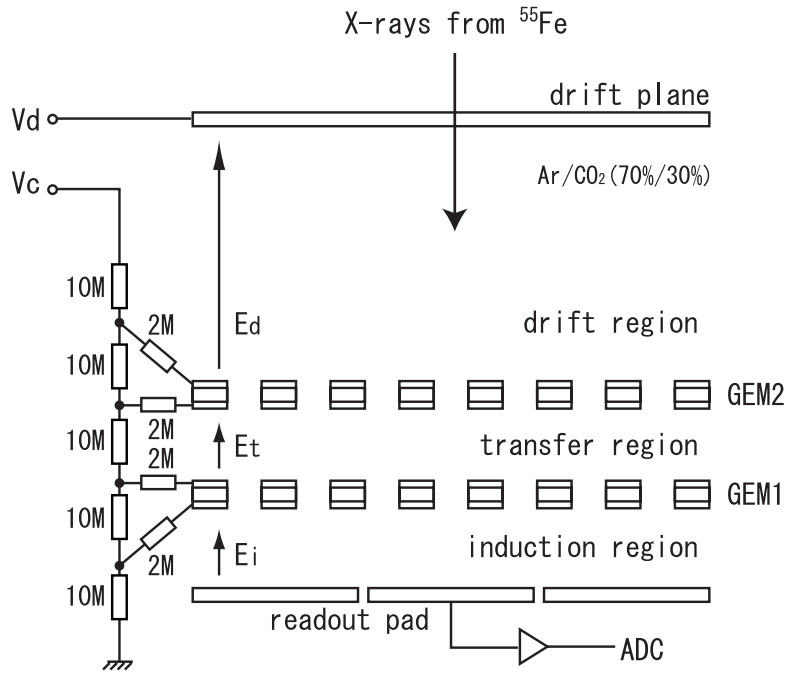
Figure 3. A schematic view of the experimental setup.

CAMAC peak-hold ADC (LeCroy 2259B) controlled by a PC. To make a calibration curve between amount of input charge and ADC channel, a well-defined rectangular wave from a research pulser (ORTEC model 448) was fed into the preamplifier through a 2pF capacitor.

During the test, we flowed a mixture of 70% argon and 30% carbon dioxide by volume through the chamber. The CO_2 sense as a quencher. The primary reason we selected this gas mixture was to easily compare our results to other experiments; many GEM studies have been done with this gas mixture. We did not add any gases to prevent discharge, aging effects, etc. in this study.

3.2. Gain of the GEMs

We have measured electron gain as a function of applied voltage between the two copper electrodes of a GEM. Since it is difficult to measure the real GEM gain in the amplification channel, we define effective gain (G_{eff}) as the ratio of detected charge to input one, and use this definition of gain throughout this paper. In this study, the effective gain is measured with 5.9 keV X-ray irradiation from a ^{55}Fe radioactive source. Note that the effects of charge losses during the electron transfer in gas, GEMs and readout pads are merged into the G_{eff} in this study.

The main peak in the ^{55}Fe spectrum corresponding to the 5.9 keV X-ray is fitted with a Gaussian to measure the central value (S_{mean}) of the peak. The effective gain is found as:

$$G_{eff} = Const \times \frac{S_{mean}}{q_e \, n_e} \tag{1}$$

where q_e is the electron charge and n_e is the number of electron-ion pairs created by the absorption of 5.9 keV X-ray. Mean value of n_e is 212 for a mixture of 70% argon and 30% carbon dioxide.[21] The constant value is found from the calibration curve between amount of input charge and ADC channel.
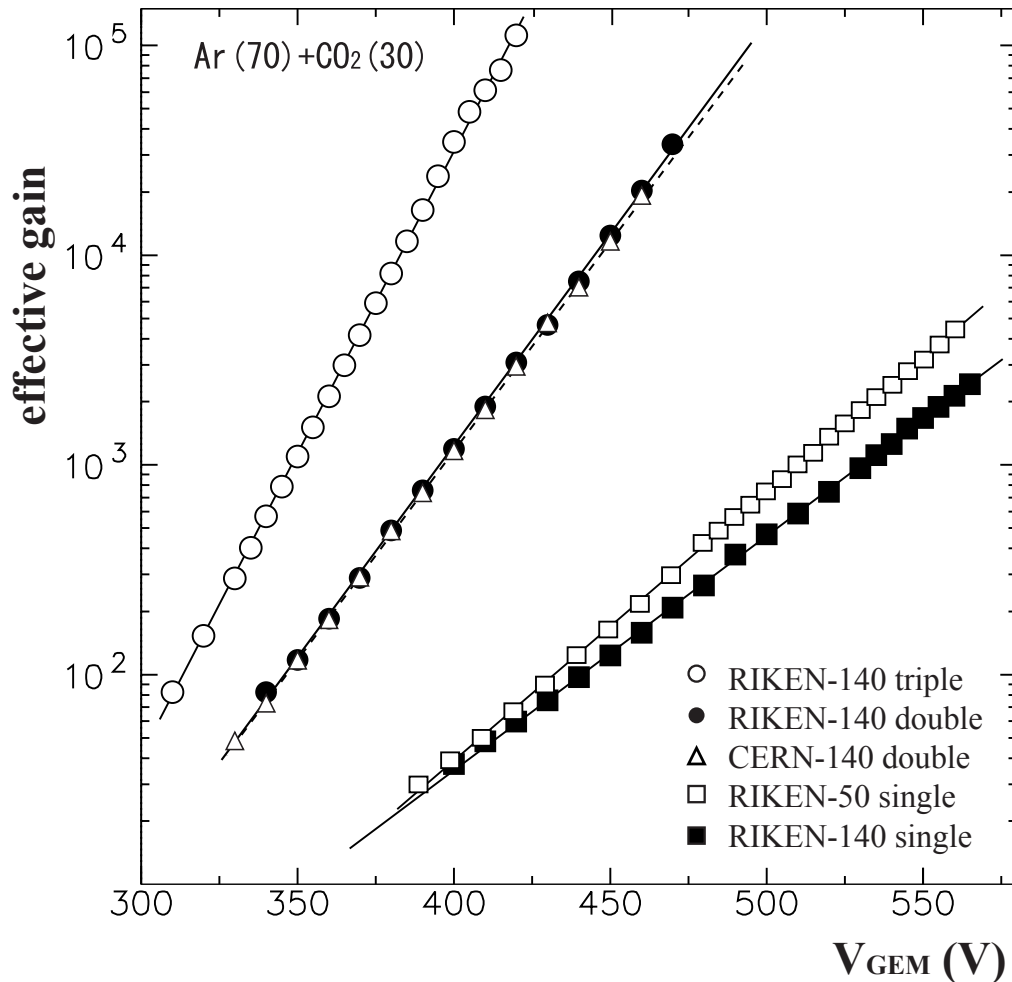
Figure 4. Effective gains of single, double and triple RIKEN-140 GEMs as a function of applied voltage between GEM electrodes. The gain of single finest-pitch GEM, RIKEN-50, is also plotted. The gain of double CERN-140 GEMs is plotted in the figure for comparison.

The effective gain of single, double, and triple RIKEN-140 GEMs are shown in Fig. 4. The effective gain of the double GEM is roughly the square of the gain of the single GEM, and that of triple GEM is roughly the cubic of the gain of the single GEM. The result of double layers of CERN-140 GEMs is also shown in the figure for comparison. The agreement between the gain curves of the CERN-140 and RIKEN-140 GEMs indicates that the gain is determined only by the geometry of the hole size and pitch. The effective gain of single RIKEN-50, which is the finest-pitch GEM we have fabricated, is also shown in Fig. 4. The gain is slightly higher than that of RIKEN-140 at the same applying voltage. This is probably due to the smaller hole diameter.

Fig. 5 shows gain properties of single layer of thick-foil RIKEN-140LCP-100T and RIKEN-140LCP-2L, which have 100 μm thickness. For comparison, gain properties of double layer of thin-foil RIKEN-140LCP's are shown in the figure. The total thickness of GEMs are the same among them. However, single layer of the thick-foil GEMs have larger gain than double layer of the thin-foil GEMs, i.e. the gain curve is steeper. An effective gas gain of 10^4 is achieved with RIKEN-140LCP-100T and RIKEN-140LCP-2L at the applied voltage of 350 V per 50 μm of thickness. The trend, thicker-foil GEM has larger gain than thin-foil one, is predicted from a simulation study done by Bouianov et al.[22] Another important character of the thick-foil GEMs is the micro-discharge voltage is considerably higher than that of the thin-foil GEMs. It is around G_{eff}=1-2$\times 10^4$ for the thick-foil
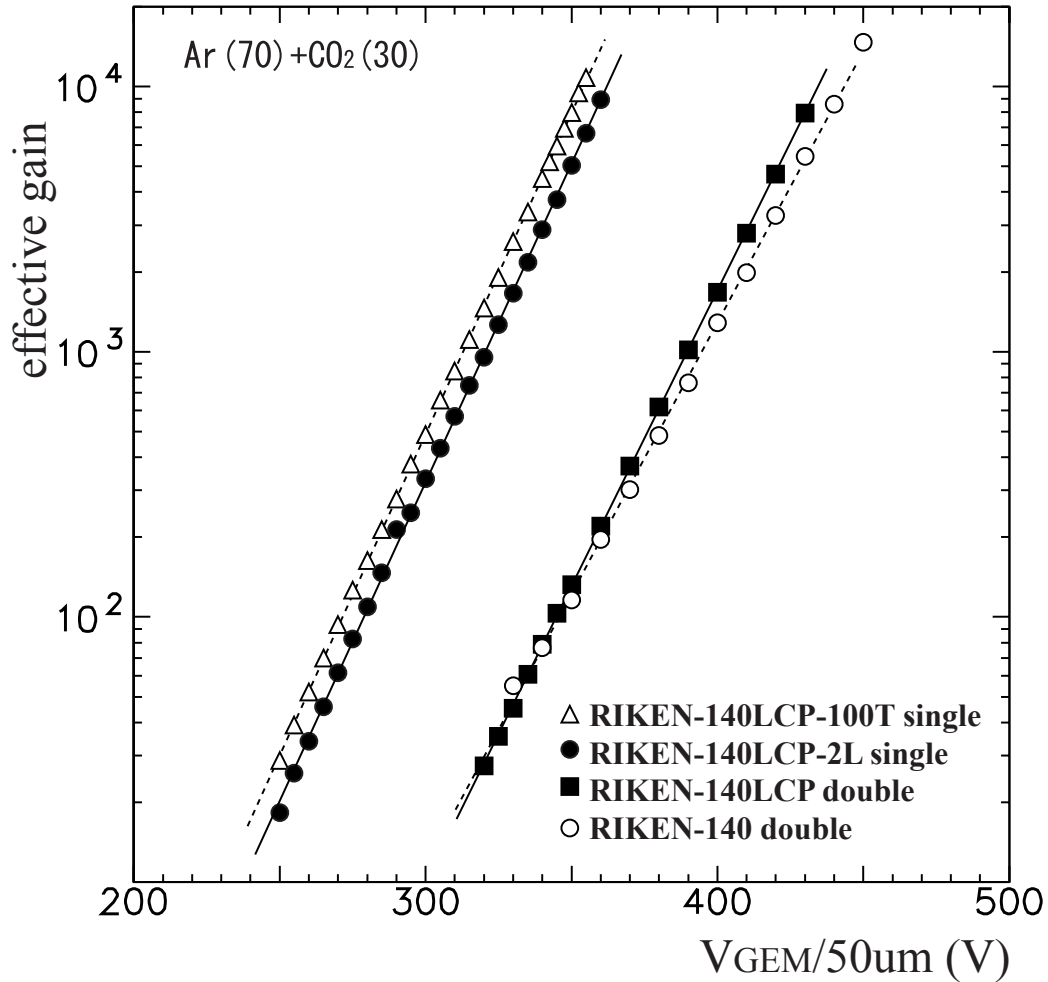
Figure 5. Figure captions are used to describe the figure and help the reader understand it's significance. The caption should be centered underneath the figure and set in 9-point font. It is preferable for figures and tables to be placed at the top or bottom of the page. LaTeX tends to adhere to this standard.

GEMs, whereas it is around G_{eff}=2-3$\times 10^3$ for single layer of RIKEN-140LCP.

Since we have used LCP as an insulator layer instead of polyimide (PI) for the first time, we have compared the gain property between them. The effective gain of double layer of RIKEN-140, which has Cu-PI-Cu foil, are shown in the Fig. 5. The gain curve of RIKEN-140LCP has steeper than that of RIKEN-140. We have no idea why the gradient of the gain curves between them at this moment. One of the possible reasons is the difference comes from the geometry of hole edge. While there is about 10° taper for the PI GEMs, there is almost cylindrical for the LCP GEMs. (See the right panel of Fig 1 and the top panel of Fig. 2.)

3.3. Electric Field of the GEMs

In Fig. 5, RIKEN-140LCP-100T has slightly higher gain than RIKEN-140LCP-2L. To study the difference, we have simulated the electric fields of them by using MAXWELL3D field simulator.[23] Since we have not calculated electron multiplication in the simulation with GARFIELD,[24] we just mention a trend of gain qualitatively. Fig. 6 shows an equipotential surface map of RIKEN-140LCP-2L and RIKEN-140LCP-100T. One can see the equipotential surface is lined-up by the middle copper layer of RIKEN-140LCP-2L, i.e. the middle metal layer works as a field shaper. On the other hand, there is no such constrained condition for RIKEN-140LCP-100T.
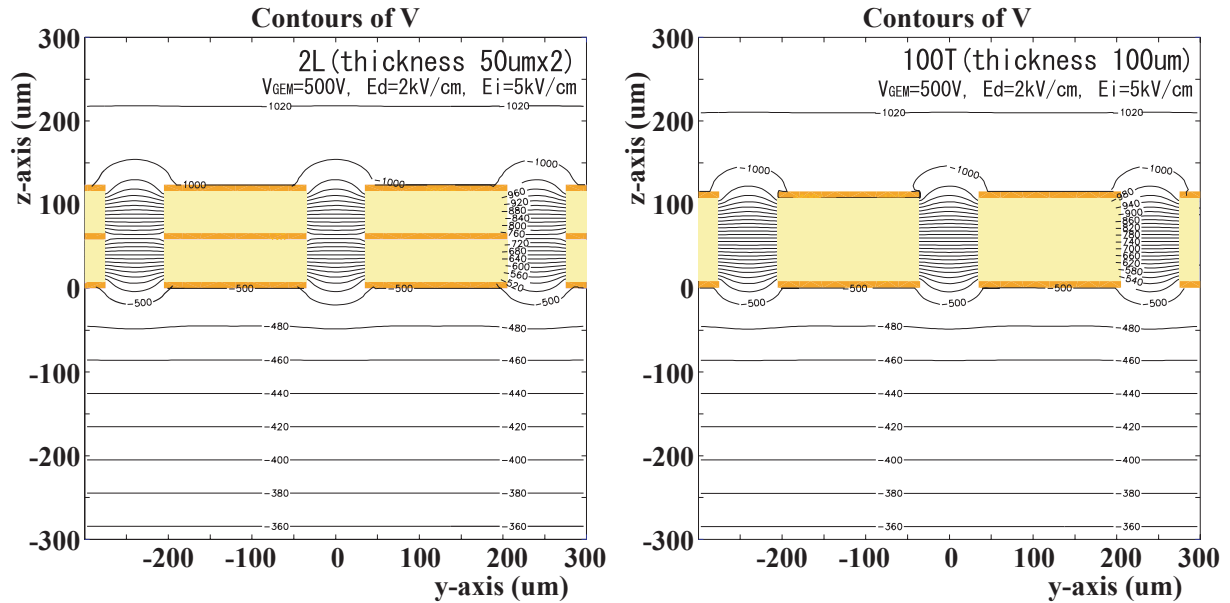
Figure 6. Equipotential surface for RIKEN-140LCP-2L (left) and RIKEN-140LCP-100T (right).

Fig. 7 shows the strength of electric field along the line perpendicular to the GEM foil for RIKEN-140LCP-2L and RIKEN-140LCP-100T. The electric field of RIKEN-140LCP-2L becomes small around the copper electrode in the middle of the layer. The effect is conspicuous along the line through the hole edge. This is why the effective gain of RIKEN-140LCP-2L is smaller than that of RIKEN-140LCP-100T. For the 100 μm-thick foil, the middle copper layer makes the effective gain worse. Since it shapes electric field in the amplification channels, the middle layer probably works better in the effective gain and prevents micro-discharge for thicker foils.

4. SUMMARY AND FUTURE WORKS

We have developed fine-pitch and thick-foil GEMs using laser etching technique for cosmic X-ray polarimeters. The minimum dimension of the GEM we have fabricated is 50 μm-pitch and 30 μm-diameter. The maximum thickness of the GEM is 100 μm.

We have measured the effective gain for 140 μm-pitch and 70 μm-diameter GEMs and 50 μm-pitch and 30 μm-diameter GEMs. The 140 μm-pitch GEM was compared to the same structure GEM fabricated by CERN, and we found that the gain property is nearly the same. The effective gain of single layer of the 50 μm-pitch GEM is slightly larger than that of 140 μm-pitch GEM due to probably the smaller hole diameter. The gain reaches about 5000 at the voltage of 570 V between electrodes.

Liquid crystal polymer (LCP) has been employed for producing thicker-foil GEMs. A gas gain of 10^4 is achieved with the 100 μm-thick GEMs at the applied voltage of 350 V per 50 μm of thickness. On the other hand, the gain of 50 μm-thick GEM is 10^2 at the same voltage. We have produced two different type of thick-foil GEMs. One of them has 100 μm-thick LCP layer sandwiched by two copper layers. The other has a middle copper layer sandwiched by two 50 μm-thick LCP layers and copper electrodes. The middle metal layer works as a field-shaper. The effective gain is, however, decreased slightly by the layer.

In the next production, we will fabricate thicker-foil GEMs with thickness of 150-200 μm. we hope they have higher gas gain than 100 μm-thick GEM, and they probably keep voltage without discharge beyond effective gain $>10^4$. We also plan to fabricate 50 μm-pitch GEM with thickness of 100 μm, and apply it to our X-ray polarimeter.[10]
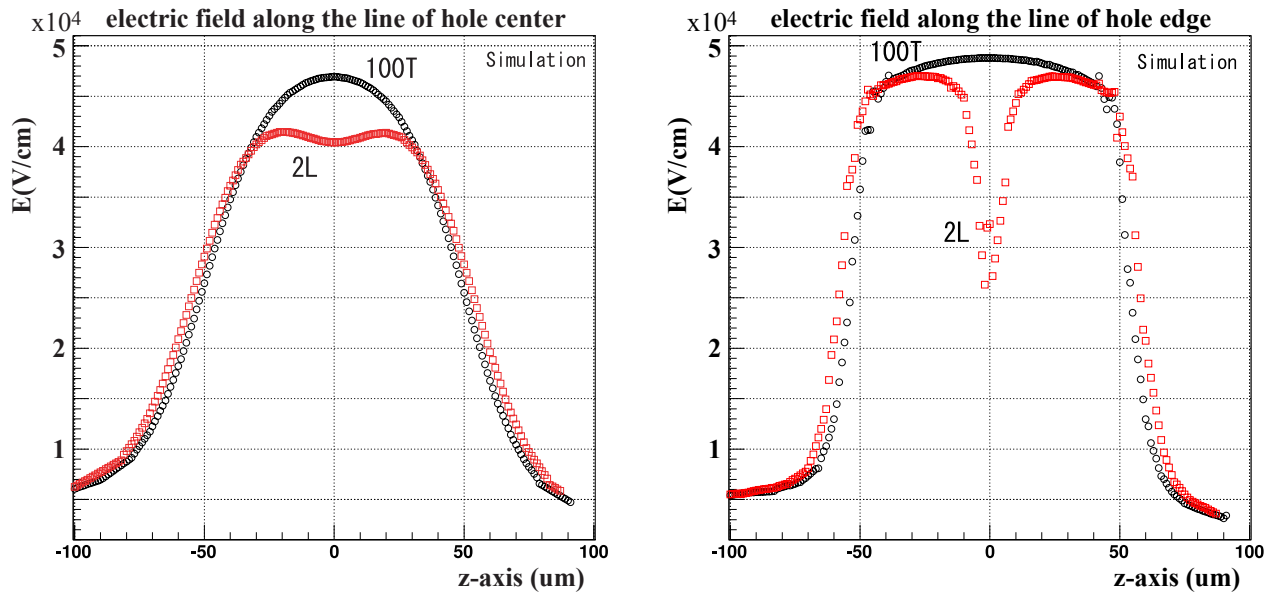
Figure 7. Electric field strength which a primary electron feels along the line perpendicular to the GEM surface and through the hole center (left), and along the line through the hole edge (right) for single layer of RIKEN-140LCP-2T and RIKEN-140LCP-100T. $V_{GEM}=500$ V.

REFERENCES

1. F. Sauli, "Gem: A new concept for electron amplification in gas detectors," *Nucl. Instrum. Meth.* **A386**, pp. 531–534, 1997.
2. S. Bachmann *et al.*, "Performance of gem detectors in high intensity particle beams," *Nucl. Instrum. Meth.* **A470**, pp. 548–561, 2001.
3. A. Buzulutskov *et al.*, "The gem photomultiplier operated with noble gas mixtures," *Nucl. Instrum. Meth.* **A443**, pp. 164–180, 2000.
4. D. Mormann, A. Breskin, R. Chechik, and C. Shalem, "Operation principles and properties of the multi-gem gaseous photomultiplier with reflective photocathode," *Nucl. Instrum. Meth.* **A530**, pp. 258–274, 2004.
5. A. Breskin *et al.*, "Ion-induced effects in gem and gem/mhsp gaseous photomultipliers for the uv and the visible spectral range," *Nucl. Instrum. Meth.* **A553**, pp. 46–52, 2005.
6. F. Sauli, "Gas detectors: Achievements and trends," *Nucl. Instrum. Meth.* **A461**, pp. 47–54, 2001.
7. E. Costa, P. Soffitta, R. Bellazzini, A. Brez, N. Lumb, and G. Spandre, "An efficient photoelectric x-ray polarimeter for the study of black holes and neutron stars," *Nature* **411**, pp. 662–665, 2001.
8. R. Bellazzini, L. Baldini, E. Costa, L. Latronico, N. Omodei, P. Soffitta, and G. Spandre, "A photoelectric polarimeter based on a micropattern gas detector for x-ray astronomy," *Nucl. Instrum. Meth.* **A510**, pp. 176–184, 2003.
9. J. K. Black, P. Deines-Jones, S. E. Ready, and R. A. Street, "X-ray polarimetry with an active-matrix pixel proportional counter," *Nucl. Instrum. Meth.* **A513**, pp. 639–643, 2003.
10. A. Hayato *et al.*, "Development of cosmic x-ray polarimeter," *Proc. SPIE* **6266**. (in this proceeding).
11. T. Tabata, R. Ito, and S. Okabe, "Generalized semiempirical equations for the extrapolated range of electrons," *Nucl. Instrum. Meth.* **103**, pp. 85–91, 1972.
12. R. Bellazzini, F. Angelini, L. Baldini, A. Brez, E. Costa, *et al.*, "X-ray polarimetry with a micro pattern gas detector with pixel read out," *IEEE Trans. Nucl. Sci.* **NS-49**, p. 1216, 2002.
13. M. Inuzuka, H. Hamagaki, K. Ozawa, T. Tamagawa, and T. Isobe, "Gas electron multiplier produced with the plasma etching method," *Nucl. Instrum. Meth.* **A525**, pp. 529–534, 2004.

14. T. Tamagawa *et al.*, "Development of gas electron multiplier foils with a laser etching technique," *Nucl. Instrum. Meth.* **A**, 2006. (in press).

15. J. Benlloch *et al.*, "Development of the gas electron multiplier (gem)," *IEEE Trans. Nucl. Sci.* **45**, pp. 234–243, 1998.

16. W. K. Pitts *et al.*, "Development and operation of laser machined microwell detectors," *Nucl. Instrum. Meth.* **A438**, pp. 277–281, 1999.

17. H. S. Cho *et al.*, "Gem: Performance and aging tests," *IEEE Trans. Nucl. Sci.* **46**, pp. 306–311, 1999.

18. CERN Gas Detectors Development Group. http://gdd.web.cern.ch/GDD/.

19. Nippon Steel Chemical Co., Ltd. http://www.nscc.co.jp/english/materials/index.html.

20. A. Bondar, A. Buzulutskov, L. I. Shekhtman, and A. Vasiljev, "Study of ion feedback in multi-gem structures," *Nucl. Instrum. Meth.* **A496**, pp. 325–332, 2003.

21. F. Sauli *CERN Yellow Report* **77-09**, 1997.

22. O. Bouianov, M. Bouianov, R. Orava, and V. Tikhonov, "Foil geometry effects on gem characteristics," *Nucl. Instrum. Meth.* **A458**, pp. 698–709, 2001.

23. Maxwell 3-D Field Simulator, User's Reference, Ansoft Corporation.

24. R. Veenhof. Garfield: A Drift-Chamber Simulation Program, Version 6.32.